Henning Bonart, André Marek, Jens-Uwe Repke

Experimental characterization of stable liquid rivulets on inclined surfaces: Influence of surface tension, viscosity and inclination angle on the interfacial area

Journal article | **Accepted manuscript (Postprint)**
This version is available at https://doi.org/10.14279/depositonce-9098

Bonart, H., Marek, A., & Repke, J.-U. (2017). Experimental characterization of stable liquid rivulets on inclined surfaces: Influence of surface tension, viscosity and inclination angle on the interfacial area. Chemical Engineering Research and Design, 125, 226–232. https://doi.org/10.1016/j.cherd.2017.07.022

Experimental Characterization of Stable Liquid Rivulets on Inclined Surfaces: Influence of Surface Tension, Viscosity and Inclination Angle on the Interfacial Area

Henning Bonart[a], André Marek[b], Jens-Uwe Repke[a]

[a] *Technische Universität Berlin, Process Dynamics and Operations Group, Str. des 17. Juni 135, 10623 Berlin, Germany*
[b] *TU Bergakademie Freiberg, Leipziger Str. 28, 09599 Freiberg, Germany*

Abstract

In this work, liquid rivulets on inclined, smooth surfaces were examined experimentally using light-induced fluorescence. The influence of viscosity, surface tension and inclination angle was studied in terms of the Reynolds and Kapitza numbers. Detailed results on the interfacial area of the rivulets were obtained. Based on the experimental results, a correlation of the interfacial area in dependence on the Reynolds and Kapitza numbers is proposed. It is found, that the correlation can reproduce the experiments very well.

Keywords: Rivulet flow, Light-induced fluorescence, Interfacial area

1. Introduction

Liquid film flow over solid surfaces are of great importance for chemical engineering applications demanding high heat and mass transfer rates. Examples include distillation and absorption processes as well as falling film reactors and reboilers. Affected by various parameters like mass flow rates, surface structures and physical properties like viscosity, the gravity driven flow down inclined plates can exhibit a range of different flow patterns. At low flow rates the liquid film tends to split into several rivulets and droplets. A rivulet is a narrow film which spreads freely on a solid surface [1]. This leads to a smaller interfacial area between the liquid flow and an overflowing

Email address: `jens-uwe.repke@tu-berlin.de` (Jens-Uwe Repke)

gas phase than widespread film flows [2]. As a consequence, the effective area for mass and heat transfer is greatly reduced.

To accurately predict the mass and heat transfer performance of rivulets, an understanding of the fluid dynamics is essential. Accordingly, a number of experimental and numerical studies have been conducted on the hydrodynamics of rivulets. First detailed experiments and calculations on straight rivulets on inclined plates were conducted by [3], in which the influence of the liquid flow rate on the rivulet's width was examined. Later on, calculations and experiments were performed for example to describe the velocity distribution in rivulets [4], the stability of rivulets [5] and the influence of curved surfaces [6]. In [7], light-induced fluorescence measurements were used to describe shape and tip speed of rivulets. The wetting behavior and rivulet formation were researched by [2] using numerical simulations and experiments. Detailed measurements of the width of rivulets on different plate materials were reported by [8] and numerical simulations and experiments on the width and thickness of rivulets were performed by [9]. In [10], the film thickness and velocity distribution of rivulets and droplets were measured using light-induced fluorescence. Numerical simulations to characterize the influence of surface textures on the wetting of plates and the formation of rivulets were conducted by [11]. Calculations on the shape of the wavy surface of rivulets were compared with existing experimental measurements in [12]. Recently, comprehensive numerical simulations were performed in [13] to calculate the interfacial area of rivulets under the variation of liquid properties, surface properties and inclination angles. However, little attention has been paid to the direct experimental characterisation of the rivulet's interfacial area.

In the present paper a new correlation for the interfacial area of rivulets based on the Reynolds number and the Kapitza number is proposed. A total of 108 distinct measurements of the interfacial area for four different fluid mixtures on a smooth, flat plate were conducted. The experiments were performed using the light-induced fluorescence method for a wide range of fluid properties and flow conditions. In this way, the influence of surface tension, viscosity, inclination angle and mass flow on the interfacial area was identified.

2. Experiments

2.1. Setup

For this contribution a new apparatus was designed to investigate the interfacial area of liquid rivulets. The measurements were conducted using light-induced fluorescence, see [7, 10, 14] for details. The experimental setup is shown in Fig. 1. The flat plate on which the rivulet was formed had a length

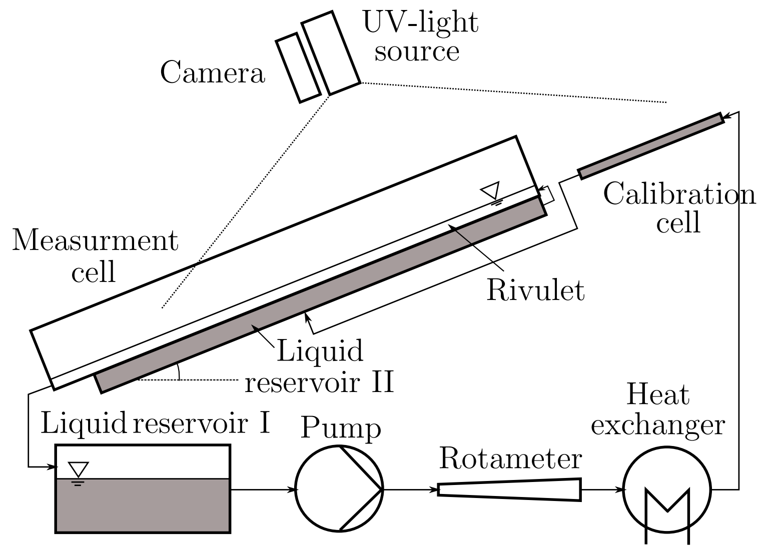

Figure 1: Experimental setup.

of 300 mm and a width of 150 mm. The width of the measurement cell was large enough to prevent contact of the rivulet with the outer walls. The plate was made of stainless steel with a surface roughness of 37 µm. The liquid inlet was constructed as a point distributor acting like an overflow weir. The measurement cell as well as the calibration cell were illuminated uniformly by a continuously operated single light source (manufacturer: igb-tech GmbH, type: FRDA202) with wavelengths from 340 nm-440 nm and peak wavelength at 395 nm. A long pass filter with 420 nm cutoff wavelength was added in front of the lens to block reflected light from other sources then the fluorescent dyes. The emitted light in both measurement and in-situ calibration cell was captured with a single 5.5 MP sCMOS camera (manufacturer: PCO AG, type: pco.edge) with an exposure time of 25 ms. In Fig. 2 a photo of the plate is displayed with a rivulet in the center and the calibration cell in the upper right corner. The light source and the camera were positioned

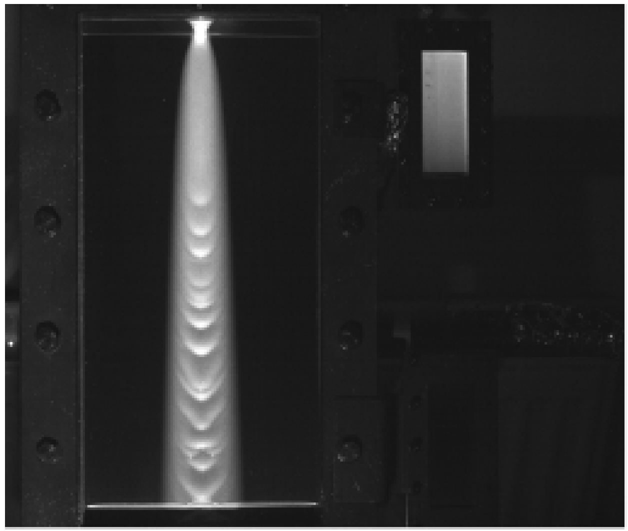

Figure 2: Photo of the light-induced fluorescence of the plate with the rivulet and the in-situ calibration cell (upper right corner). Brightness of the image is enhanced for better visibility.

orthogonal to both the measurement cell and the calibration cell. The height inside the calibration cell increased linear from 0.3 mm to 2.0 mm to represent several liquid film thicknesses, see Fig. 3. The whole setup was installed into

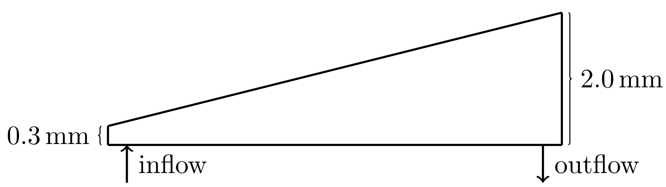

Figure 3: Side view of the in-situ calibration cell.

a single frame with all components fixed at defined positions. The frame with all components was inclined to the horizontal in its entirety. In this way, accurate measurements for different inclination angles were ensured.

2.2. Performed Experiments

The used liquids and dyes are listed together with their measured physical properties in Tab. 1. Triton X-102 was used as the surfactant. The contact angles of the fluids were measured using the sessile drop method. Note, that it is not easily possible to vary the surface tension of a liquid without varying

Identifier	Dye	Density ρ (kg/m^3)	Surf. tension σ (mN/m)	Dyn. viscosity η (mPa s)	Contact angle θ (°)	Ka[a]
DC10[b]	Coumarin 152	940	18	10.419	27	36
DC5[b]	Coumarin 152	920	18	5.073	30	91
Water/Surfactant[b]	Fluorescein	998	29	1.114	53	1150
Water[c]	Fluorescein	998	72	1.178	79	2070

[a] Kapitza number with inclination angle $\alpha = 90°$, see Eqn. 3 for details.
[b] Dow Corning 200 with different viscosities
[c] Deionized water

Table 1: Physical properties of the examined liquids measured at 25 °C.

its contact angle using the same surface. As a consequence, the liquids and the surface were chosen such that the contact angles were at least in a narrow range over all experiments. Tab. 2 lists the examined Kapitza and Reynolds numbers used in the performed experiments. The measurements were performed with the four different mixtures each at nine different flow rates and three different inclination angles (60°, 75°, 90°). In total, 108 distinct configurations were probed. For the present experiments, the gas phase above the rivulet was stagnant. The temperature of the liquid was held constant at 25° C. Coumarin 152 (max. excitation wavelength 395 nm, max. emission wavelength of 510 nm) and Fluorescein (max. excitation wavelength 490 nm, max. emission wavelength of 520 nm) were used as the fluorescence dyes with a concentration of about 50 mg/l in conjunction with the silicon oils respectively the aqueous systems. Note, that while the maximum excitation wavelength of Fluorescein is not found near the peak wavelength of the light source (as it is the case for Coumarin 152), sensitive measurements using Fluorescein were still possible due to the high sensitivity of the dye and its wide excitation spectrum. In this work, the whole setup was flushed and rinsed before every single experiment. Then the measurement cell was flooded with the fluid using a high inlet mass flow to fully wet the surface. Afterwards, the inlet mass flow was slowly adjusted to the target mass flow. After a stable rivulet was formed, the remaining droplets and liquid accumulations without any connection to the rivulet were carefully removed from the plate by hand. In this way, the conditions on the flat surface were very well reproducible and the risk of a meandering rivulet was low.

DC10	Ka	37.7	36.4	36.0						
	Re	0.3	1.1	1.9	2.8	4.4	7.2	11.9	19.3	30.7
DC5	Ka	96.1	92.6	91.6						
	Re	1.0	3.3	5.9	9.0	14.7	24.0	38.3	59.6	90.0
Wat./Surf.	Ka	1207.4	1164.2	1150.9						
	Re	29.6	72.8	141.9	193.1	269.8	372.2	500.1	653.6	832.7
Water	Ka	2172.2	2094.6	2070.5						
	Re	27.2	76.5	127.1	176.1	249.8	347.9	470.6	617.9	789.6

Table 2: Values of the examined Kapitza (Eqn. 3) and Reynolds numbers (Eqn. 2).

2.3. Post-processing

The recorded photos were automatically post-processed using custom made scripts for the computing environment *Matlab*. As proposed in [10] a photo without any liquid was subtracted per pixel from the images. In this way, the grey-level offset from zero fluorescence intensity as well as background color inhomogeneities were reduced. Furthermore, it was recognized during the post-processing, that subtracting a background image from the pictures could lower the reflections from the plate surface. Afterwards, *Matlab's* spatial filter function was applied with a circular averaging filter of radius 7 pixel to reduce the noisy character of the light-induced fluorescence measurements.

The per picture obtained grey levels in the calibration cell were matched with their corresponding heights or film thicknesses. For every picture, a second order polynomial was fitted through the matched values to obtain a smooth calibration function, see Fig. 4. The calibration functions were linearly extrapolated to grey values representing film thicknesses below the minimal height of the calibration cell, i.e., below 0.33 mm. In this way, the spatially distributed thickness of the rivulet was obtained and the rivulet was extracted from the background. By using this in-situ calibration measurement per picture errors due to changes of incoming light intensity and dye concentration were reduced. Finally, the interfacial area was calculated from the geometric properties of the rivulets by:

$$A_{if,exp} = \delta x \sum_{i=1}^{NC-1} \sum_{j=lb(i)}^{rb(i)} \sqrt{{\delta y_{i,j}}^2 + {\delta h_{i,j}}^2}\ , \qquad (1)$$

in which $\delta y_{i,j}$ is the distance between the points $y_{i,j}$ and $y_{i,j+1}$ at the ith cut perpendicular to the flow direction and $\delta h_{i,j}$ is the difference of the rivulet's thickness at these points. lb and rb of the index j at the ith cut are the left respectively right bound of the rivulet, δx is the distance between two cuts i and NC is the total number of horizontal lines between upper and lower edges of the plate. By using this procedure the interfacial area of the rivulets could be reliably determined from light-induced fluorescence measurements.

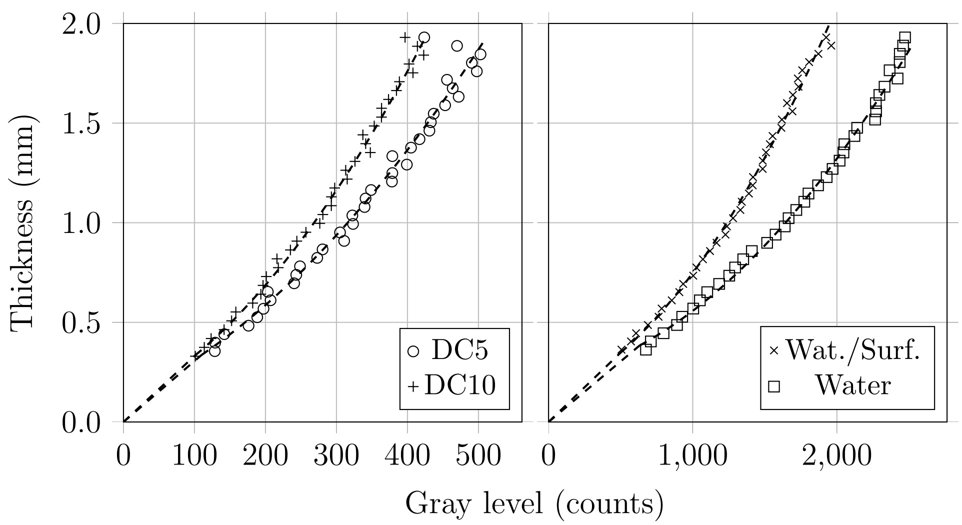

Figure 4: Exemplarily calibration plots for the different liquids and dyes.

3. Results and Discussion

Fig. 5 shows light-induced fluorescence recordings of the liquids at low (top) and high Reynolds numbers or flow rates (from left to right: DC5, DC10, Wat./Surf., Water). The inclination angle of the plate was 60°. It is clearly visible, that all rivulets spreaded on the plate and exhibited a certain entrance flow length. For the silicon oils DC5 and DC10, the spreading was not finished by the end of the plate, whereas water/surfactant reached a steady width in the first few centimeters after the inlet. As seen in the photos, the water rivulets were the most unstable at both low and high Reynolds numbers. At low Reynolds numbers, the water rivulet tended to meander on the plate, whereas at high Reynolds numbers a steady rivulet, but with increasing and decreasing widths, was formed. Furthermore, waves started to occur for the silicon oils at high Reynolds numbers.

In the following, the spatial properties width and thickness of the rivulets are presented. The thickness was averaged over the horizontal axis or width of the rivulet. Based on the experimental values, a correlation for the interfacial area was identified. The discussion as well as the identified model are based on the Reynolds Re and Kapitza Ka numbers:

$$Re = \frac{4 \cdot \dot{V} \cdot \rho}{U \cdot \eta} \tag{2}$$

$$Ka = \sigma \cdot \left(\frac{\rho}{\eta^4 \cdot \sin(\alpha) \cdot g} \right)^{1/3} , \tag{3}$$

with the volumetric flow rate $\dot{V}$, the perimeter of the inlet U, the inclination angle of the plate α and the gravitational acceleration g as well as the fluid properties density ρ, dynamic viscosity η and surface tension σ. The usage of the Kapitza number is advantageous, because it combines the important fluid properties density, viscosity and surface tension. It is constant for a given fluid but depends on the current inclination angle. A detailed analysis of the dimensions can be found in [15].

3.1. Thickness and Width

The Figs. 6 and 7 display the width respectively the horizontally averaged thickness. The Kapitza number rises from the top to the bottom of the figures and the Reynolds number rises in every single plot from the bottom to the top. The inclination angle rises from the left to the right. The corresponding values of the Kapitza number and the Reynolds number are given in Tab. 2. The results show a strong dependency of the wetted width as well as the average thickness on both the Reynolds and Kapitza numbers. The shown values were averaged using between two (silicon oils) and five (aqueous systems) photos of the same rivulet and the error bars are the deviation from the mean. For high values of the Kapitza number the width is nearly constant along the flow length. In contrast, the width increases along the flow length for low values of Ka. The width of the silicon oils increases continuously over the flow length for all values of Re. For water/surfactant a slight decrease for the lowest Re and an increasing wetted width for the highest Re over the flow length occurs. Using water, the wetted width as

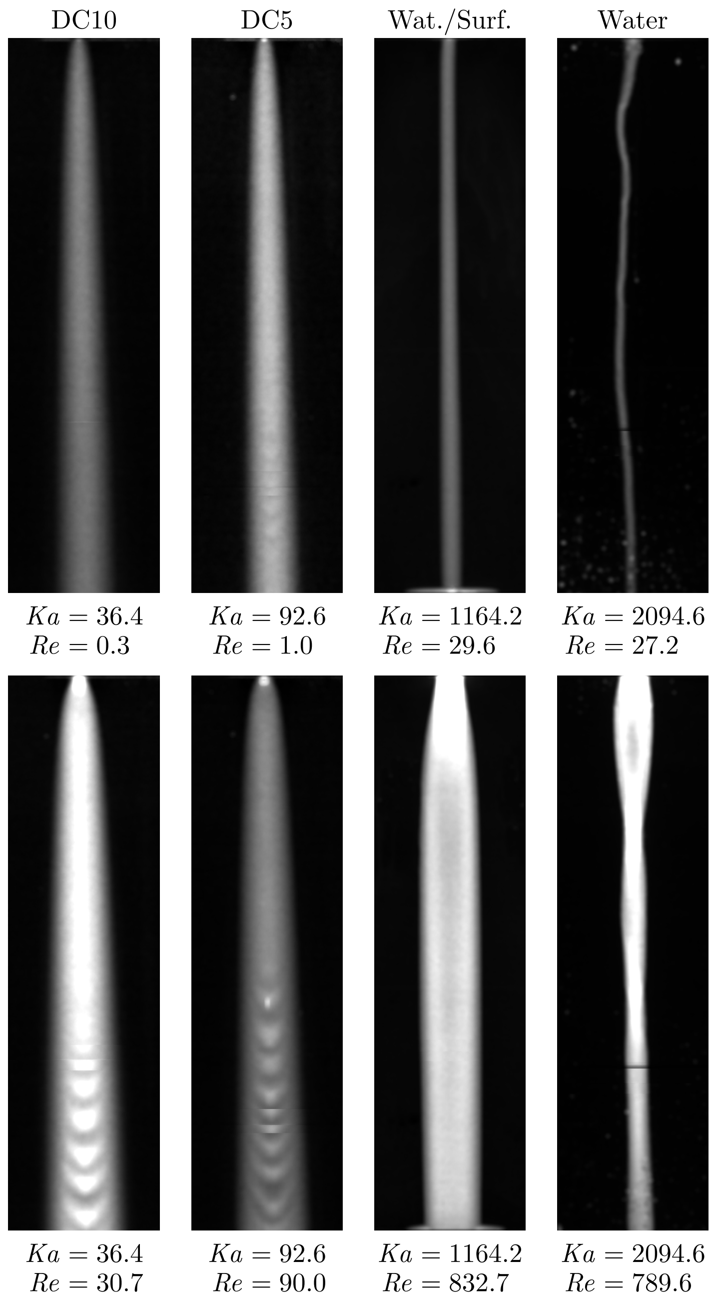

Figure 5: Light-induced fluorescence recordings of the rivulets at low (top) and high Reynolds numbers (from left to right: DC5, DC10, Wat./Surf., Water). The inclination angle of the plate is 60°. Brightness of the image is enhanced for better visibility.

well as the averaged thickness tend to decrease and reflect the oscillating character already reported by [16].

The geometries of the rivulets show general trends in dependence on the flow rate, inclination angle and fluid properties. With higher values of Re both width and thickness increase for all fluids and inclination angles. A contrary behavior is observed for higher values of Ka. Consistent to [17], the width is reduced for rising values of Ka for all fluids and inclination angles. The thicknesses on the other hand shows a more complex dependency. The thickness is greatly reduced for rising Ka but gets to higher values again for very high Ka (water). In the whole range of Reynolds and Kapitza numbers, the width is reduced for higher inclination angles. This was already reported by [7] and [13].

3.2. Interfacial Area

Based on the local measurements of thickness and width, the interfacial area $A_{if,exp}$ of the rivulets were reconstructed as described in section 2. All experimental results were combined into a single correlation. The interfacial areas obtained from the experiments were fitted using *fitnlm*, which is part of the *Statistics and Machine Learning Toolbox* of *Matlab*. This resulted in the following proportionality[1] for the interfacial area $A_{if,corr}$:

$$A_{if,corr} \sim \frac{Re^{1/5}}{Ka^{1/3}} \ . \tag{4}$$

A similar scaling has been recently observed in numerical simulations by [13].

Fig. 8 shows the correlation 4 against the experimental values. It is visible from the correlation, that the interfacial area rises with higher Reynolds numbers. On the other hand, large Kapitza numbers decrease the interfacial area. This agrees with the general trends observed in subsection 3.1 for the width and thickness. The correlation matches most of the experimental data in the entire parameter range within ±30%, as shown in Fig. 8. For high values of Ka (pure water) the deviation is slightly larger. The overall

[1]The measured contact angles (see Tab. 1) are not incorporated into the correlation yet, see subsection 2.2 and the conclusion 4.

normalized root-mean-square deviation given by:

$$NRMSD = \sqrt{\frac{\sum_{i=1}^{n}(A_{if,exp,i} - A_{if,corr,i})^2}{n}} / (\max(A_{if,exp}) - \min(A_{if,exp})) \ , \quad (5)$$

with n equals the total number of experimental values, is $NRMSD = 0.12$. As a result, the correlation can be reliably used to compute the interfacial area of rivulets for a wide range of the Reynolds number Re (0.3-800) and the Kapitza number Ka (36-2170).

4. Conclusion

The interfacial area between rivulets and surrounding gas is an important parameter for applications in chemical engineering like distillation and absorption processes as well as falling film reactors. In this study, the influence of surface tension, viscosity, inclination angle and mass flow on the interfacial area of liquid rivulets was investigated experimentally. A total of 108 distinct measurements of the interfacial area for four different fluids were conducted using light-induced fluorescence measurements. The results showed a strong dependency on the mass flow and the fluid properties. Subsequently, a new correlation based on the Reynolds number and Kapitza number was developed. The correlation was found to accurately predict the experimental values. The results of this study provide a convenient possibility for the validation of detailed numerical simulations as well as for the development of advanced models used for the design of film reactors or column packages. In future experiments, the influence of the surface tension and the contact angle on the interfacial area will examined separately using different plate materials and surfaces.

References

References

[1] G. Q. Wang, X. G. Yuan, K. T. Yu, Review of mass-transfer correlations for packed columns, Industrial and Engineering Chemistry Research 44 (23) (2005) 8715–8729. doi:10.1021/ie050017w.

[2] A. Hoffmann, I. Ausner, J.-U. Repke, G. Wozny, Fluid dynamics in multiphase distillation processes in packed towers, Computers & Chemical Engineering 29 (6) (2005) 1433–1437. doi:10.1016/j.compchemeng.2005.02.004.

[3] G. D. Towell, L. B. Rothfeld, Hydrodynamics of rivulet flow, AIChE Journal 12 (5) (1966) 972–980. doi:10.1002/aic.690120524.

[4] I. M. Fedotkin, G. A. Mel'nichuk, F. F. Koval', E. V. Klimkin, Hydrodynamics of rivulet flow on a vertical surface, Journal of Engineering Physics 46 (1) (1984) 9–14. doi:10.1007/BF00826157.

[5] P. Schmuki, M. Laso, On the stability of rivulet flow, Journal of Fluid Mechanics 215 (1990) 125–143.

[6] B. R. Duffy, H. K. Moffatt, Flow of a viscous trickle on a slowly varying incline, The Chemical Engineering Journal and The Biochemical Engineering Journal 60 (1-3) (1995) 141–146. doi:10.1016/0923-0467(95)03030-1.

[7] M. F. G. Johnson, R. A. Schluter, M. J. Miksis, S. G. Bankoff, Experimental study of rivulet formation on an inclined plate by fluorescent imaging, Journal of Fluid Mechanics 394 (1999) 339–354. doi:10.1017/S0022112099005765.

[8] A. Gajewski, Contact angle and rivulet width hysteresis on metallic surfaces. Part I: With heated surface, International Journal of Heat and Mass Transfer 51 (25) (2008) 5762–5771. doi:10.1016/j.ijheatmasstransfer.2008.05.019.

[9] H. Lan, J. L. Wegener, B. F. Armaly, J. A. Drallmeier, Developing laminar gravity-driven thin liquid film flow down an inclined plane, Journal of Fluids Engineering 132 (8) (2010) 81301. doi:10.1115/1.4002109.

[10] T. Hagemeier, M. Hartmann, M. Kühle, D. Thévenin, K. Zähringer, Experimental characterization of thin films, droplets and rivulets using LED fluorescence, Experiments in Fluids 52 (2) (2012) 361–374. doi:10.1007/s00348-011-1232-x.

[11] D. Sebastia-Saez, S. Gu, P. Ranganathan, K. Papadikis, 3D modeling of hydrodynamics and physical mass transfer characteristics of liquid film

flows in structured packing elements, International Journal of Greenhouse Gas Control 19 (0) (2013) 492–502. doi:10.1016/j.ijggc.2013.10.013.

[12] S. Alekseenko, S. Aktershev, A. Bobylev, S. Kharlamov, D. Markovich, Nonlinear forced waves in a vertical rivulet flow, Journal of Fluid Mechanics 770 (2015) 350–373. doi:10.1017/jfm.2015.170.

[13] R. K. Singh, J. E. Galvin, X. Sun, Three-dimensional simulation of rivulet and film flows over an inclined plate: Effects of solvent properties and contact angle, Chemical Engineering Science 142 (2016) 244–257. doi:10.1016/j.ces.2015.11.029.

[14] M. Isoz, Study of the rivulet type flow of the liquid on the inclined plate, Master thesis, Institute of Chemical Technology Prague and TU Bergakademie Freiberg (2013).

[15] S. Kalliadasis, C. Ruyer-Quil, B. Scheid, M. G. Velarde, Falling Liquid Films, Vol. 176 of Applied Mathematical Sciences, Springer London, London, 2012. doi:10.1007/978-1-84882-367-9.

[16] T. M. S. Nakagawa, R. Nakagawa Jr., A Novel Oscillation Phenomenon of the Water Rivulet on a Smooth Hydrophobic Surface, Acta Mechanica 7 (1-4) (1996) 27–37. doi:10.1007/BF01187426.

[17] M. G. Shi, A. Mersmann, Effective interfacial area in packed columns, German chemical engineering 8 (2) (1985) 87–96.

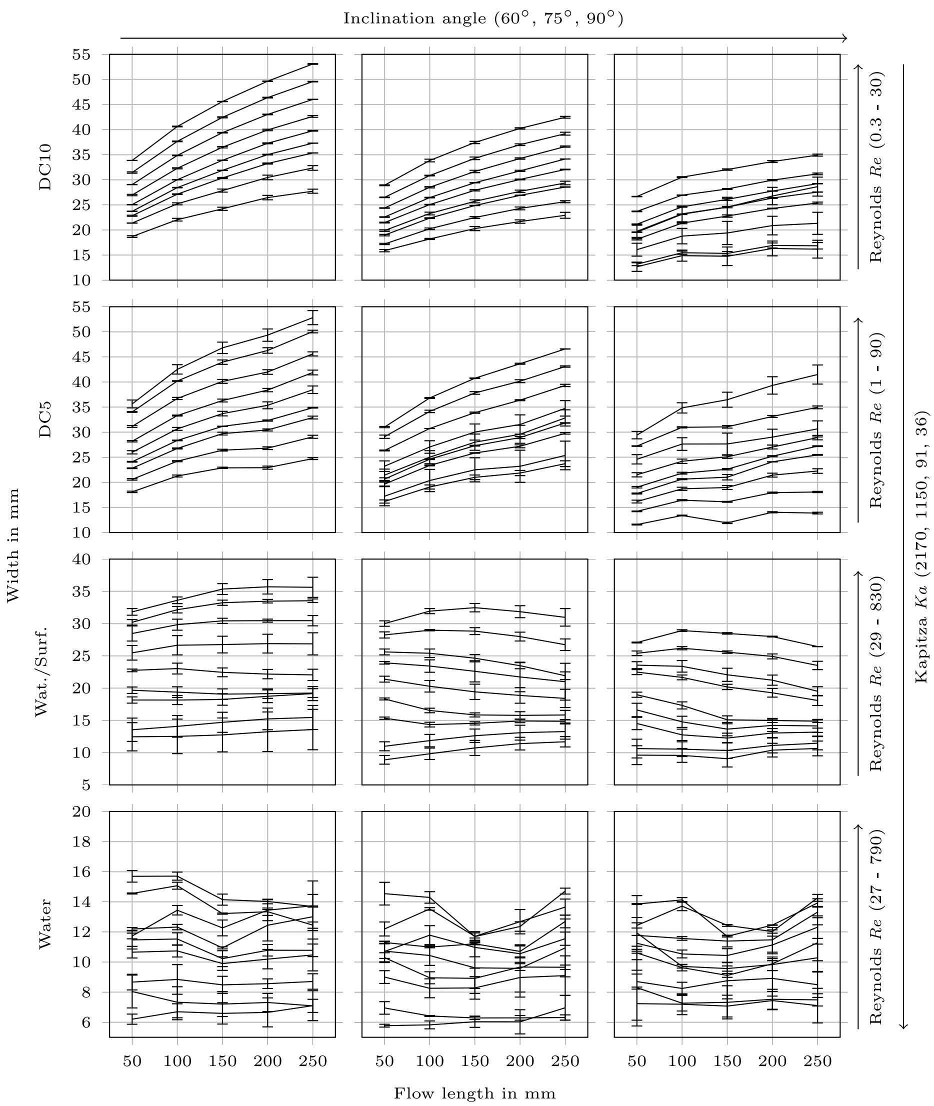

Figure 6: Width of the rivulets over flow length.

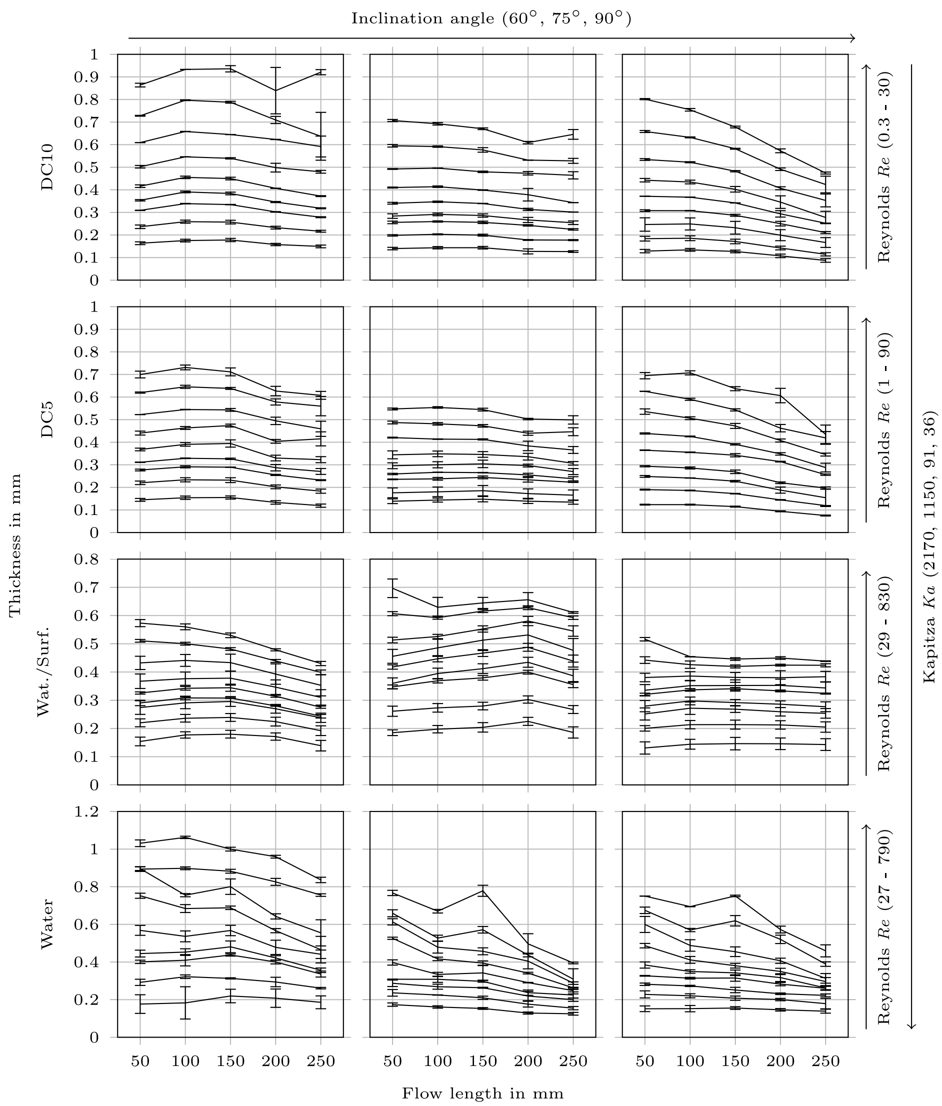

Figure 7: Averaged thickness of the rivulets over flow length.

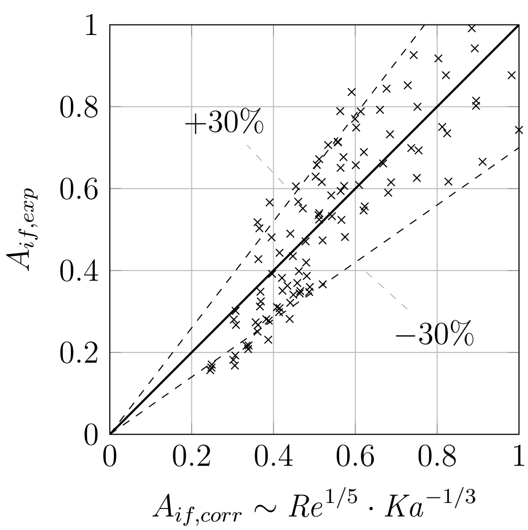

Figure 8: Correlation of the interfacial area for the entire investigated parameter range ($0.324 < Re < 800$, $36 < Ka < 2170$, $60°$ to $90°$) against the experimental values. All values are normalized with the maximal interfacial area.